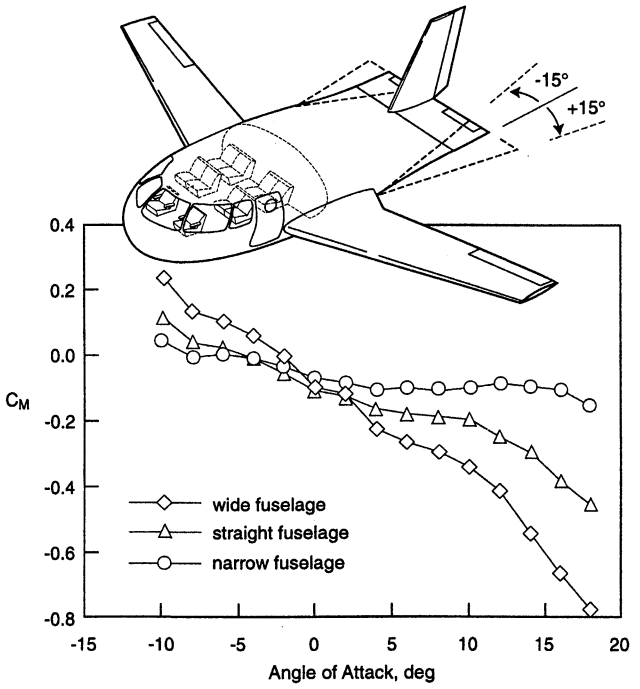

Fig. 5 Effect of aft-fuselage taper on pitching moment (Re = 0.4 × 10^6, scale 1:20).

loring of the sudden increase in the pitching-moment slope into a desirable angles-of-attack range. Therefore, when an airplane's c.g. calculations and elevator sizing are complete, the use of these data can make airplane stall unreachable.

Concluding Remarks

The experimental data presented here indicate that a small aircraft with a wide lifting-body fuselage can benefit, in addition to the large cabin size, from several unique aerodynamic features. The configuration can reach quite high lift coefficients because of the fuselage vortex lift, without sacrificing the L/D at low angles of attack. The high-angle-of-attack vortex lift at the aft section of the fuselage causes a large nose-down pitching moment, which can be utilized for a stall-safe design. Finally, the basic principle of using the fuselage as a simple and cheap high-lift device was demonstrated.

Acknowledgment

The authors wish to thank Stig Johansson for his help in designing, building, and testing the wind-tunnel model.

References

[1]Cantilli, E. J., "Saga of the Lifting Body/Flying Wing," *Flight Journal*, Vol. 1, No. 2, 1996, pp. 56–61.

[2]*Jane's Encyclopedia of Aviation*, Vol. 2, Jane's Information Group, Ltd., Coulsdon, Surrey, UK, 1980, p. 367.

[3]Mitchell, K. A., "Burnelli and His Lifting-Body Transports," *American Aviation Historical Society Journal*, Spring 1997, pp. 2–19.

[4]Liebeck, R. H., Page, M. A., and Rawdon, B. K., "Blended-Wing-Body Subsonic Commercial Transport," AIAA Paper 98-0438, Jan. 1998.

[5]Hahl, R., and Katz, J., "Lifting-Fuselage/Wing Aircraft Having an Elliptical Forebody," U.S. Patent Appl. 08-642997, May 13, 1996.

[6]Raymer, D. P., *Aircraft Design: A Conceptual Approach*, AIAA Educational Series, AIAA, Washington, DC, 1992, Chap. 12.

[7]Katz, J., Byrne, S., and Hahl, R., "Stall Resistance Features of Lifting-Body Airplane Configurations," AIAA Paper 98-0760, Jan. 1998.

Application of Active Separation Control to a Small Unmanned Air Vehicle

A. Seifert,* T. Bachar,† and I. Wygnanski‡
Tel-Aviv University, Tel-Aviv 69978, Israel
and
A. Kariv,§ H. Cohen,¶ and R. Yoeli**
Aero Design and Development, Inc., Rehovot 76102, Israel

Introduction

THE delay of boundary-layer separation by oscillatory injection of momentum established the superiority of the method over steady blowing.[1] The performance of various airfoils was improved, even when separation was not entirely avoided. Although the addition of small amounts of steady blowing to the fluctuating momentum slightly reduces the efficiency of the excitation, the application of steady blowing may require two orders of magnitude greater momentum coefficient for similar gains in performance. While most wind-tunnel experiments used external devices to excite the flow, a self-contained system is required for active flow control in flight. Furthermore, mounting an active flow control device on an unmanned air vehicle (UAV) or an airplane model allows one to test its effectiveness as an alternate control surface. This Note describes wind-tunnel experiments on a UAV to which active separation control was added to improve its performance and to exercise roll authority in an unconventional manner.

Approach

The project was subdivided into four intermediate stages:

1) The application of oscillatory and steady blowing to a flapped Eppler 214 airfoil. The oscillatory blowing was initially provided by an external mechanism.[2] Some of the results were presented in Ref. 1 and they will not be discussed here.

2) The development of a self-contained oscillatory blowing system.

3) The installation of the system on the UAV and full-scale tests in a low-speed, industrial wind tunnel.

4) Actual flight tests of the UAV with active separation control.

The quantitative results obtained during stage 3 are reported in this Note.

Experiment

A scaled down Scout UAV was used in the experiment, but its original wing was replaced with a wing based on the Eppler 214 airfoil of a larger span. A simply hinged, 30% chord, trailing-edge flap and ailerons spanned the outer section of the

Received July 8, 1998; revision received Aug. 31, 1998; accepted for publication Sept. 15, 1998.

*Engineer, Fluid Mechanics and Heat Transfer Department; currently on leave from Tel-Aviv University, National Research Council Researcher, NASA Langley Research Center, M/S 170, Hampton, VA 23681. Member AIAA.

†Engineer, Department of Fluid Mechanics and Heat Transfer.

‡Professor, Fluid Mechanics and Heat Transfer Department; also AME Department, University of Arizona, Tucson, AZ 85721. Fellow AIAA.

§Aerodynamic Project Manager.

¶Team Leader, System Engineering.

**Managing Director.

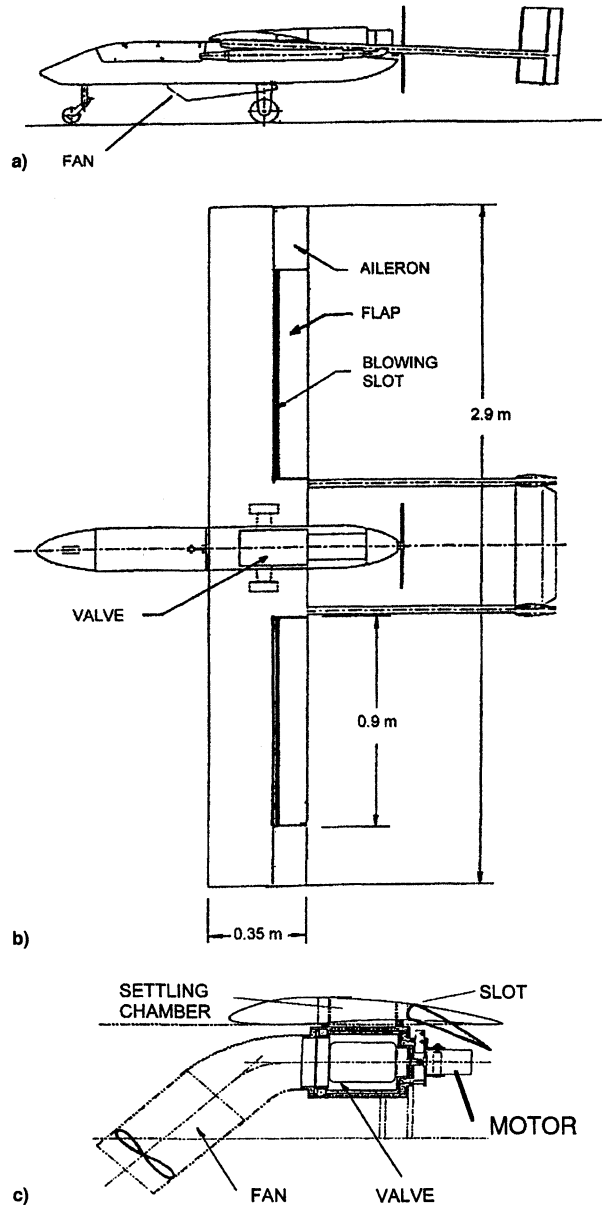

Fig. 1 a) Side and b) top views of the modified, 1:2 scale Scout UAV, and c) side view of the fan–valve–wing assembly.

wing beyond the tail booms (Figs. 1a and 1b). The entire UAV was made of composite materials, its maximum takeoff weight was 16 kg, and its wing area was 1.015 m^2. The stalling speed of this UAV was 13 m/s, when its flaps were not deployed. Other dimensions are given in Fig. 1.

The excitation system consisted of a rotating valve and an axial fan mounted inside the fuselage. The inlet of the fan was on the underside (Fig. 1). The rotating valve provided the oscillations by redirecting the steady fan-flow from one wing to another at a frequency of 50–70 Hz. These frequencies were found to be the most effective over the range of Reynolds numbers considered, generating a reduced frequency $F^+ = fc_f/U_\infty$ of 0.5–0.7, where f is the excitation frequency, c_f is the flap chord, and U_∞ is the flight speed. About 30% of the wing volume was taken up by the internal duct. The oscillatory blowing emanated from slots, 0.9 mm high, located at the flap shoulders (Fig. 1). The calibration of the oscillatory blowing was done using a single hot wire located at the slot exit in the absence of external flow. The procedure was repeated at 18 discrete locations along each slot. Typical rms levels of the velocity fluctuations were 3–4 m/s, whereas the steady jet component was 7–10 m/s. These values generated a combined blowing momentum coefficient[1] of

$$C_\mu = (2hb_f/SU_\infty^2)(U_j^2;\ u'^2) = (0.18;\ 0.03)\%$$

where the first number signifies the steady component and the second number is the oscillatory one. Here, b_f is the total spanwise extent of the active slots, whose height is h, and S is the wing area. U_j is the averaged jet velocity, whereas u' is its rms level. Although only the flow above the flaps was controlled, the active slot area was normalized by the entire wing area to retain the conventional meaning of the momentum coefficient. The system was recalibrated while the slot over one wing was sealed, to estimate the contribution of the active flow control to the rolling moment. In this case, the resulting excitation was $C_\mu = (0.08;\ 0.015)\%$. The tests were carried out in the 3.6 by 2.6 m, Israel Aircraft Industries low-speed wind tunnel that operates at airspeeds of 5–100 m/s. The model was mounted on an external balance through its three landing gear struts after its wheels were removed. No attempt was made to account for wall interference, and so the data can only be used to assess the relative improvement in performance resulting from the application of active separation control. The resolution of the wind-tunnel balance is about 0.5% of the minimum drag measured. External power was provided to the fan and valve motors to extend the test duration, while caution was exercised to avoid loading the balance. The valve and fan were remotely controlled by radio. The UAV was equipped with a side-mounted, angle-of-attack indicator that was also calibrated during these tests.

Results

The results for chord Reynolds number, $Re_c = 0.27 \times 10^6$ (12 m/s), provide the baseline data for the application of the oscillations. The reduced frequency was $F^+ = 0.7$, and a momentum coefficient of $C_\mu = (0.18;\ 0.03)\%$ was applied over both flaps. Three flap deflection angles were tested: $\delta_f = 0$, 20, and 30 deg. The baseline lift coefficients are marked in Fig. 2 by dashed lines. As expected, the maximum lift coefficient, $C_{L,\max}$, increased with increasing flap deflection while the stall angle decreased. The linear $C_L - \alpha$ dependence breaks down at $\alpha > 6$ deg for $\delta_f = 0$ deg. Active separation control (solid lines) is beneficial, even at $\delta_f = 0$ deg, where linear $C_L - \alpha$ was maintained up to $\alpha = 8$ deg, and $C_{L,\max}$ was increased by 0.10. This is because the excitation delayed the upstream creep of flow separation from the trailing edge. At $\delta_f = 20$ deg, the control applied over the separated flap generated a lift incre-

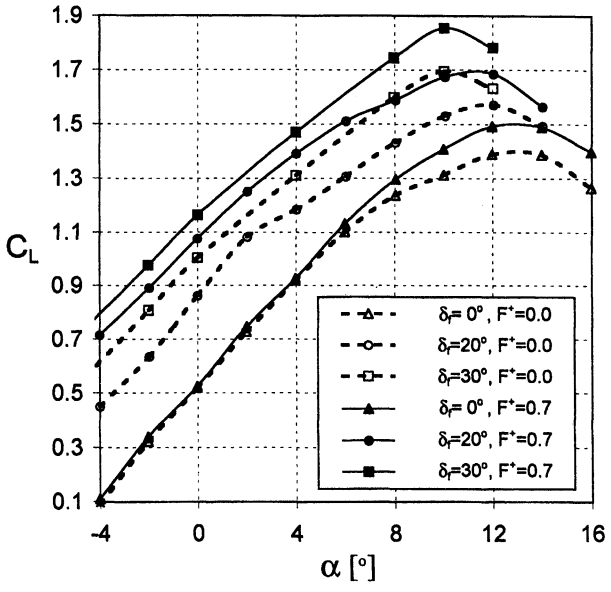

Fig. 2 UAV lift vs angle of attack.

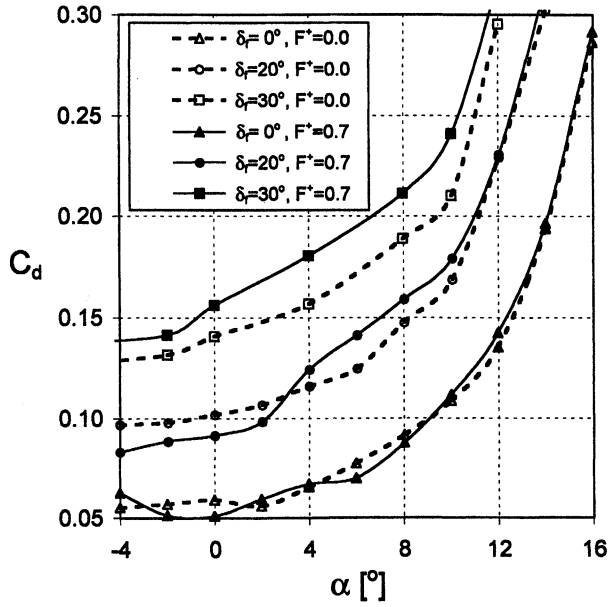

Fig. 3 UAV drag vs angle of attack.

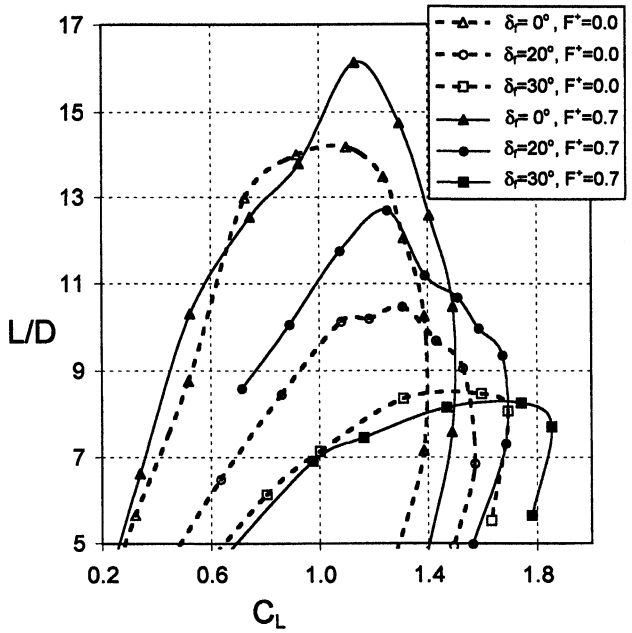

Fig. 4 UAV *L/D* vs lift.

ment (ΔC_L) of 0.25 at $\alpha = -4$ deg that decreased to $\Delta C_L = 0.2$ at $\alpha = 6$ deg and 0.12 at $C_{L,\max}$. The smaller lift increment near $C_{L,\max}$ was more clearly observed during the airfoil tests,[1] and was attributed to incomplete reattachment of the flow. Later experiments on a generic flap configuration[3] indicated that the addition of steady blowing at $C_\mu < 0.18\%$ was actually detrimental to flow reattachment by oscillatory means (see Fig. 11 in Ref. 2 for a NACA 0015 data). At $\delta_f = 30$ deg, the available blowing mechanism generated a $\Delta C_L = 0.15$ throughout the entire α range, suggesting that the flow was not entirely reattached owing to the application of the active control. The fact that the stall angle was not affected by excitation is another indication that flow separation originated on the flap; it resulted in a decrease of the $C_L - \alpha$ slope. When the separation location moved upstream of the flap, the actuation was not effective.

The $C_D - \alpha$ plots shown in Fig. 3 indicate that drag was decreased whenever flow separation was prevented in a significant way. This is most clearly demonstrated at $\delta_f = 20$ deg, where for $\alpha \leq 2$ deg, the increase in lift was accompanied by a concomitant reduction in drag. For 2 deg $< \alpha <$ 12 deg, a relative increase in drag was observed despite the increase in lift. This is a result of partially separated flow over the flap, stemming from a combination of steady blowing and low F^+ used. An increase in skin friction may have been caused by enhanced entrainment upstream of the slot,[2] which mainly contributed to the enhancement of lift. For $\delta_f = 30$ deg, both lift and drag have increased at all angles of incidence examined. The drag coefficient of the fuselage alone (with wings, tail booms, and stabilizers removed) at identical R_c was approximately 0.023, decreasing slightly with increasing α. The estimated uncertainty in the drag measurement is ± 0.0025.

A plot of *L/D* vs C_L is given in Fig. 4. It shows an increase in the maximum *L/D* of $2 \approx C_L$ at 1.1 and 1.3 (corresponding to $\delta_f = 0$ and 20 deg, respectively), and it represents an improvement of ~20% at the higher C_L. The oscillatory blowing used did not improve the glide ratio, i.e., *L/D*, at the high flap deflection of $\delta_f = 30$ deg; thus, the optimum improvement in the performance of the configuration tested is limited to $5 > \delta_f > 15$ deg.

The rolling moment coefficient (C_R) created by the asymmetric excitation of the flow over a single flap is plotted in Fig. 5. Both flaps were deflected at $\delta_f = 20$ deg, whereas only the flow over the left flap was perturbed at $F^+ = 0.7$ and $C_\mu = (0.08; 0.015)\%$. The perturbations generated $C_R \approx 0.02$, without the use of ailerons. The C_R generated by deflecting the ailerons to their limit was $C_R \approx 0.035$ (while $\delta_f = 0$ deg). Because C_R is a product of the local change in lift and the spanwise location of the aileron relative to the longitudinal axis, it is estimated that the local changes in lift coefficients caused by the periodic blowing and by the maximum aileron deflection were comparable. These data suggest that an airplane can be controlled by introducing perturbations into the flow rather than moving control surfaces. The replacement of classical ailerons by active flow control devices does not have the familiar adverse yaw effects.

The results of the experiments described herein demonstrate the application of active separation control to a UAV using a self-contained perturbation system. No unexpected situations were encountered as a result of the application of active flow control to a part of the wingspan. The lift measured by using a balance on the full UAV was reasonably well estimated from previous, two-dimensional tests. The use of an active aileron that does not require the motion of a conventional control surface was also demonstrated.

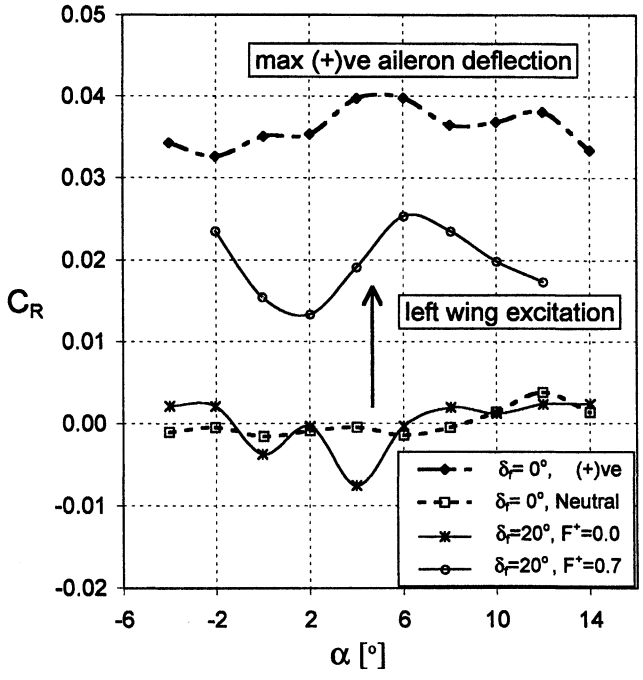

Fig. 5 UAV rolling moment caused by left wing excitation.

Acknowledgments

This manuscript was written while the first author held a National Research Council–NASA Langley research fellowship. Support from the staff and contractors of Aero Design and Development, Inc., is appreciated. Thanks also go to A. Darabi and S. Eliahu from Tel-Aviv University, and M. Livne, the former manager of the wind-tunnel center at Israel Aircraft Industries.

References

[1]Seifert, A., Darabi, A., and Wygnanski, I. "On the Delay of Airfoil Stall by Periodic Excitation," *Journal of Aircraft*, Vol. 33, No. 4, 1996, pp. 691–699.

[2]Seifert, A., Bachar, T., Koss, D., Shepshelovich, M., and Wygnanski, I., "Oscillatory Blowing, a Tool to Delay Boundary Layer Separation," *AIAA Journal*, Vol. 31, No. 11, 1994, pp. 2052–2060.

[3]Nishri, B., and Wygnanski, I., "Effects of Periodic Excitation on Turbulent Flow Separation from a Flap," *AIAA Journal*, Vol. 36, No. 4, 1998, pp. 547–556.

Inviscid Interactions Between Wake Vortices and Shear Layers

Z. C. Zheng* and K. Baek†
University of South Alabama, Mobile, Alabama 36688-0002

Introduction

AIRCRAFT trailing vortices can be influenced significantly by atmospheric conditions such as crosswind, turbulence, and stratification. According to the NASA 1994 and 1995 field measurement program in Memphis, Tennessee,[1] the descending aircraft wake vortices could stall or be deflected at the top of low-level temperature inversions that usually produce pronounced shear zones.

Numerical simulations of vortex/shear interactions with ground effects have been performed by several groups.[2–5] Burnham[6] used a series of evenly spaced line vortices at a particular altitude to model the ground shear layer of the crosswind. He found that the wind shear was swept up around the downwind vortex and caused the downwind vortex to move upward, and claimed that the effect was actually produced by the vertical gradient in the wind shear rather than by the wind shear directly, because uniformly distributed wind-shear vortices would have no effect on the trailing vortex vertical motion. Recently, Proctor et al.[7] numerically tested the effects of narrow shear zones on the behavior of the vortex pair, motivated by the observation of the Memphis field data. The shear-layer sensitivity tests indicated that the downwind vortex was more sensitive and deflected to a higher altitude than its upwind counterpart. The downstream vortex contained vorticity of opposite sign to that of the shear. There was no detectable preference for the downwind vortex (or upwind vortex) to weaken (or strengthen) at a greater rate.

The preceding observations indicate that the mechanism responsible for the asymmetric deflection in the trailing vortices can possibly be deduced from inviscid interactions between the vortex pair and shear layers. Based on that hypothesis, a vortex method model is developed to study that mechanism. Furthermore, this vortex method is much faster than the Navier–Stokes numerical simulations, and thus can be used for real-time predictions.

Model Description

For the two-dimensional flow considered here, the Cauchy kernel integral for the Biot–Savart velocity can be obtained for the Lagrangian-type point vortex method used in this study.[8] In the current model, the primary trailing vortex pair is represented by two opposite sign point vortices. A shear layer is modeled by placing a layer of vortices, with constant circulation. Figure 1a shows an example of the initial distribution of vortices for simulating interactions between the trailing vortex pair and a narrow shear zone. The vortices in the shear layer are of the same sign as the left vortex in the vortex pair. To reduce end effects at the two ends of the shear layer,

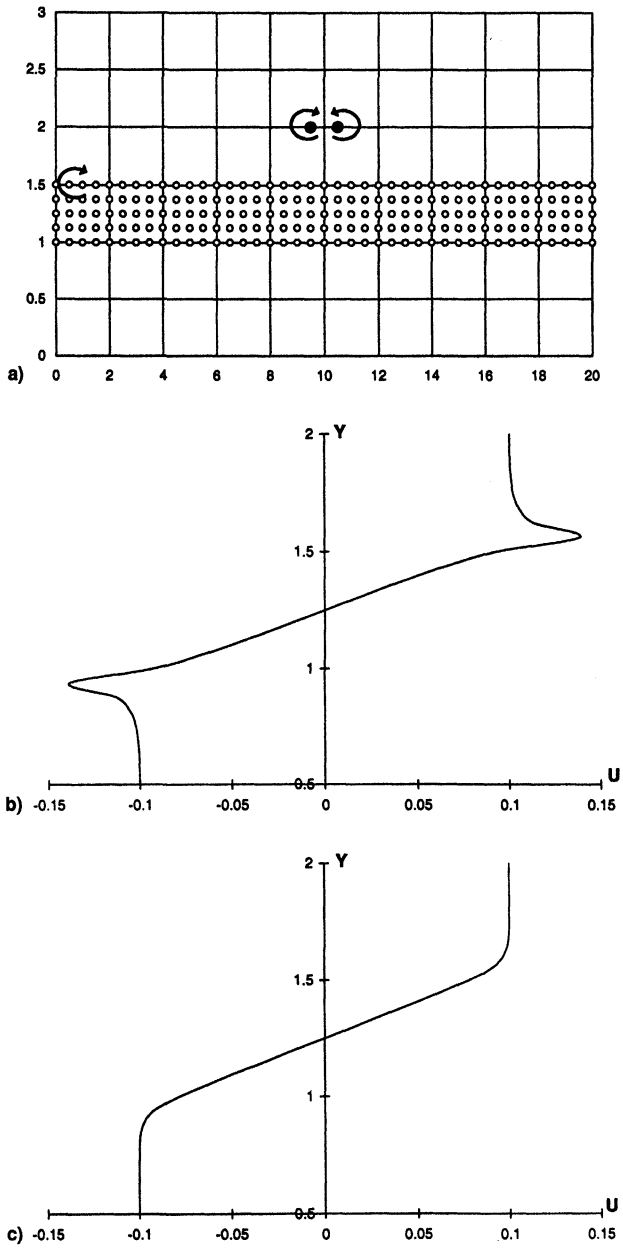

Fig. 1 Initial flowfield: a) Vortex positions. ● = the two vortices in the vortex wake, and ○ = the vortices in the shear layer. b) Velocity in x direction, u, vs height, y, at x locations aligning on the shear vortices. c) Velocity in x direction, u, vs height, y, at x locations between the shear vortices.

Received May 28, 1998; revision received Nov. 4, 1998; accepted for publication Nov. 6, 1998.

*Assistant Professor, Mechanical Engineering Department. Member AIAA.

†Graduate Research Assistant, Mechanical Engineering Department.